catalysts

MDPI

Review

Biomass-Derived Carbon Anode for High-Performance Microbial Fuel Cells

Jamile Mohammadi Moradian [1,2], Songmei Wang [1], Amjad Ali [3], Junying Liu [1], Jianli Mi [2,*] and Hongcheng Wang [1,*]

[1] Biofuels Institute, School of the Environment and Safety Engineering, Jiangsu University, Zhenjiang 212013, China
[2] Institute for Advanced Materials, School of Materials Science & Engineering, Jiangsu University, Zhenjiang 212013, China
[3] Research School of Polymeric Materials, School of Materials Science & Engineering, Jiangsu University, Zhenjiang 212013, China
* Correspondence: jlmi@ujs.edu.cn (J.M.); hcwang2870@foxmail.com (H.W.)

Abstract: Although microbial fuel cells (MFCs) have been developed over the past decade, they still have a low power production bottleneck for practical engineering due to the ineffective interfacial bioelectrochemical reaction between exoelectrogens and anode surfaces using traditional carbonaceous materials. Constructing anodes from biomass is an effective strategy to tackle the current challenges and improve the efficiency of MFCs. The advantage features of these materials come from the well-decorated aspect with an enriched functional group, the turbostratic nature, and porous structure, which is important to promote the electrocatalytic behavior of anodes in MFCs. In this review article, the three designs of biomass-derived carbon anodes based on their final products (i.e., biomass-derived nanocomposite carbons for anode surface modification, biomass-derived free-standing three-dimensional carbon anodes, and biomass-derived carbons for hybrid structured anodes) are highlighted. Next, the most frequently obtained carbon anode morphologies, characterizations, and the carbonization processes of biomass-derived MFC anodes were systematically reviewed. To conclude, the drawbacks and prospects for biomass-derived carbon anodes are suggested.

Keywords: biomass; MFCs; power output; carbon anode; nanocomposite; porous anode; exoelectrogens

check for updates

Citation: Moradian, J.M.; Wang, S.; Ali, A.; Liu, J.; Mi, J.; Wang, H. Biomass-Derived Carbon Anode for High-Performance Microbial Fuel Cells. *Catalysts* **2022**, *12*, 894. https://doi.org/10.3390/catal12080894

Academic Editors: Mohd Rafatullah, Yang-Chun Yong and Syed Zaghum Abbas

Received: 16 July 2022
Accepted: 11 August 2022
Published: 13 August 2022

Publisher's Note: MDPI stays neutral with regard to jurisdictional claims in published maps and institutional affiliations.

Copyright: © 2022 by the authors. Licensee MDPI, Basel, Switzerland. This article is an open access article distributed under the terms and conditions of the Creative Commons Attribution (CC BY) license (https://creativecommons.org/licenses/by/4.0/).

1. Introduction

Green energy production and transmitting technologies have been intensively researched to address the issues posed by pollutants and excessive fossil fuel consumption [1]. Bioelectrochemical systems (BESs), including microbial electrolysis cells (MECs) and microbial fuel cells (MFCs), owing to their mild operating conditions and wide range of organic waste degradation (electron donor), have great promise for biosensing, wastewater treatment and renewable energy generation [2–6]. Among them, MFCs contribute to more than 80% of BESs [7]. However, the low power performance and poor energy conversion of MFCs due to the sluggish interfacial bioelectrochemical reaction between exoelectrogens and anode surfaces (electron acceptors) induced by low electroconductivity of cell membrane/wall surfaces [6,8,9] and also those using traditional carbonaceous materials remain a critical hurdle in their practical engineering [7,10,11]. In previous investigations, wiring up of exoelectrogens with conducting nanoparticles (e.g., FeS, polymers, CNTs, etc.) was reported as one of the biotic/abiotic effective solutions to improve the electrochemical performance [6,8,9,12]. The traditional anode materials used in MFCs can be classified as carbon-based anodes (e.g., carbon cloth (CC) [13,14], carbon felt (CF) [15], graphene [16,17], polyaniline [18,19], etc.) and metal-based anodes (e.g., stainless steel [20] and nickel foam sheet [21], among others) [11,22]. These widely used traditional anode

materials are costly (ranging from \$50 m^{-2} to over \$1000 m^{-2}), and further, the electroactive capacity of these anode materials is relatively limited, leading to low organic waste loading along with less exoelectrogen adherence and, further owing to their restricted electrochemical characteristics, resulting in a poor extracellular electron transfer (EET) rate and high ohmic resistance [23]. To enhance the power output and optimal waste treatment in MFCs, fabricating effective anodic materials is essential to stimulate biofilm growth and EET performance.

Nanopore structured anodes with a large surface area are preferred since they can provide sufficient sites for exoelectrogens loading, enable faster ionic diffusion, aid substrate delivery, waste reduction, and minimize the clogging of anodes [11,24]. Thus, constructing anodes from renewable biomass as low-cost, highly biocompatible, and conductive materials for microbial attachment is an effective strategy to tackle the current challenges and improve the efficiency of MFCs. Lu et al. reported that the cost of a carbonized silk cocoon anode (at 900 °C for 3 h under N_2 gas flow) was approximately 50% less than the cost of a CC anode, indicating more benefits for developing MFC applications [25]. Most biomass materials have a naturally occurring porous structure that enhances the beneficial surface area for microbial attachment compared to a smooth surface, resulting in a larger electroactive surface area for optimal electron transfer [26]. For example, Karthikeyan et al. used corn stems to fabricate porous carbonaceous structured anodes for MFCs. The derived, highly electroactive biofilm on the corn carbon anode, due to the advantages of macroporous efficiently, promoted the EET kinetics of biofilm with a higher oxidative current density, about eight times higher compared to traditional plate graphite anode [22]. In another study, a hierarchically structured anode using chestnut shells based on a microscopic/macroscopic three-dimensional (3D) urchin-shaped structure could deliver a higher surface area (48.12 ± 0.83 m^2 g^{-1}) for enriched biofilm attachments with an enhanced power output of 759 ± 38 mW m^{-2}, comparable to traditional graphite brush anodes [27]. Considering the outstanding performance of biomass-derived carbon anodes for power enhancement in MFCs, this review article summarizes the types of biomass-derived carbons. Further, based on the nature of the biomass, the influence of different morphologies of biomass precursors, with their exceptional electrochemical performance in MFCs, are highlighted. Additionally, the significant strides in the fabrication strategies, with their pros and cons, are reviewed. Finally, the challenges and future trends for biomass-derived carbon anodes are provided.

2. Biomass-Derived Carbon Anodes

2.1. Biomass-Derived Nanocomposite Carbon for Anode Surface Modification

The surface modification of traditional anode materials was found to be an effective technique for enhancing MFC performance since it affected the physical and chemical characteristics of the anode electrodes with enlarged surface areas to facilitate dense exoelectrogen adhesion and faster electron transfer [28,29]. Natural biomass-derived carbon has a hierarchical and interconnected porous structure, and it can assist ionic diffusion in the anode, along with biofilm proliferation and immobilization [30]. It was reported that the distinct physicochemical features of crop and forest residue biomass, owing to plenty of organic components and a small number of inorganic elements, can develop porous carbon anodes [31]. The carbon in green plants derives from photosynthesis through carbon dioxide fixation, and the heteroatom contents (i.e., N, O, S, and P/B) are intimately associated with the enzymes involved in photosynthesis under sunlight [30]. In particular, N groups with electron-donor characteristics provide electroactive sites and optimize the electrical conductivity, surface polarity, and hydrophilicity of carbon anode surfaces by introducing defects and shifting the valence orbital energy densities of carbon atoms for enhanced electrochemical kinetics [25,32]. Nevertheless, N-doping of carbon anode surfaces can be obtained from N-containing biomass or N-containing chemicals (e.g., ammonia, polyaniline (PANI), and polypyrrole (PPy)) [32]. The enriched carbon and N contents in organic components aid self-N-doping in the carbon network to boost conductivity and

alter the surface wettability in the carbon anode, whereas inorganic elements after the carbonization phase followed by an activation procedure can serve as porogens to form nanopores, including micropores and mesopores, which accelerate the charge transfer rate between the anode surface and exoelectrogenic biofilms [26,30,31]. A wide variety of renewable biomass ranging from natural plant biomass to marine wastes and domestic and industrial wastes could be used to fabricate natural conductive nanocomposite carbon for MFCs. However, the characteristics of biomass-derived conductive nanocomposite carbon, such as morphology, specific surface area, porous structure, heteroatom doping, graphitization rate, and defects, can directly influence the electrochemical behavior and efficiency of MFCs [33]. It was reported that the CC anode modified by coffee waste-derived activated carbon (CWACs) nanocomposites exhibited a high proportion of the pseudographitic structure, with a large range of macropores and some mixed meso/micro-porous [34], referring to the disordered turbostratic nanodomains with graphitic layers. A few consistently and arbitrarily organized defects advantageous for increased ion storage sites between graphitic layers and improved diffusion kinetics [35]. Unlike the high specific surface areas in commercial activated carbons (ACs) (832.06 m^2 g^{-1}), compared to CWACs (428 m^2 g^{-1}), the maximum power density of CWAC (3927 mW m^{-2}) anodes could be obtained higher than that of the commercial AC (975 mW m^{-2}) anodes, which revealed the significance of the macroporosity structure for suitable surface roughness and increased *Escherichia coli* attachment [34]. In another study, Wang et al. reported that recycled tire crumbs coated with graphite paint could be employed as MFC anodes instead of using fine carbon materials such as graphite granules. Although the designed tire crumb anodes showed 10 times higher specific surface area (4.5 m^2 g^{-1}) compared to graphite granules (0.3 m^2 g^{-1}), it resulted a lower power density of 421 mW m^{-2} in the tire anodes and a higher power density of 528 mW m^{-2} in the graphite granule anodes. Meanwhile, the density of crumb rubber (1.1 g cm^{-3}) was much less than that of the graphite (2.2 g cm^{-3}). Although the low density of crumb rubber posed a light weight anode for reduced clogging potential, it resulted in a loose packing that hampers electrical conductivity in MFCs [36].

Nevertheless, the use of binding agents (e.g., PTFE and PVDF, among others), due to high hydrophobic and electrochemical inactivity and self-agglomeration properties, can precipitate and reduce the interfacial interface between active carbons and binder, resulting in a low anode conductivity, high ohmic resistance, and reduced MFC performance. Table 1 depicts biomass-derived conductive nanocomposite carbon for MFC anode surface modification.

Table 1. Biomass-derived conductive nanocomposite carbon for MFC anode surface modification.

Composite Anode	Structural Characteristic	MFCs Type	Anode Reactor Size	Inoculum	Power Output	Refs.
Tire crumb rubber	Light weight characteristic for reduced clogging	Single-chamber	250 mL	Anaerobic sludge	421 mW m^{-2}	[36]
Aerobic activated sludge	Disordered sheet structures	Single-chamber	100 mL	Wastewater	2165 mW m^{-2}	[37]
Candle soot	Hierarchically porous with graphitic structure	Double-chamber	50 mL	*Escherichia coli*	1650 mW m^{-2}	[38]
Almond shell	Hierarchical porous structure	Double-chamber	100 µL	Wastewater	4346 mW m^{-2}	[39]
Cocklebur fruits biochar	Clogging-resistant loose structure	Single-chamber	450 mL	Anolyte of another single-chamber MFCs	0.572 mW m^{-3}	[40]
Silver grass-derived activated carbon	Hierarchical porous structure	Double-chamber	250 mL	*E. coli*	963 mW cm^{-2}	[41]

Table 1. *Cont.*

Composite Anode	Structural Characteristic	MFCs Type	Anode Reactor Size	Inoculum	Power Output	Refs.
Lotus leaves	Hierarchical structured N, P-codoped	Single-chamber	28 mL	Activated anaerobic sludge	511.5 mW m^{-2}	[42]
Forestry residue (BCc), Milling residue (BCp)	Biochar	Double-chamber	200 mL	Anaerobic sludge	457 mW m^{-2} (BCc), 532 mW m^{-2} (BCp)	[43]
Mango wood	N/A	Single-chamber	50 mL	Effluent from MFCs	589.8 mW m^{-2}	[44]

2.2. Biomass-Derived Free-Standing Three-Dimensional Carbon Anodes

Two-dimensional (2D) porous carbon anodes with deficient macroscale pores allow biofilm to grow only on the exterior surfaces of electrodes, reducing anode efficiency [45]. Although 3D porous carbon anodes with larger specific surface areas provide more exoelectrogen colonization, resulting in a faster mass electron transport with increased ion diffusion, they are potentially beneficial for improved MFCs performance [7,28]. Nevertheless, some limitations of certain 3D structured carbonaceous materials (e.g., CF, carbon brush (CB), granular carbon, etc.), such as hydrophobic properties, low specific surface area, and too-small pore sizes for cell infiltration severely restrict the practical engineering of MFCs [45]. For example, the growth of biofilm on the surface of CF, despite its high thickness, prevents substrate passage from the outside to the inside, thereby clogging the surface, indicating the interior anode is undesirable for microbial colonization. Therefore, the inefficient use of internal area may materialize anodes of a moderate specific surface area [7].

Recent advancement in materials science engaging natural biomass has received growing interest, mainly in its porous nature and robust electrocatalytic conductivity [46]. Most biomass has a rich pore structure and integrated microchannels that make up its inherently ordered porous structure [33]. It has been suggested that a strategically tuned free-standing and hierarchically porous carbon anodes with pore diameters of <10 nm are beneficial for electrocatalytic activity [21,24,47]. Accordingly, carbon anodes with macroporous architectures (>2 μm) enable exoelectrogens penetration in the interior of the anode, but microporous carbon anodes can facilitate the diffusion of endogenous electron shuttles (e.g., riboflavin) to improve EET kinetics [28]. In natural biomass, depending on the type of plant body that is affecting the metabolic functions and water transportation, the range of pore size of carbon anodes might be different [22]. In a study by Zhang et al., the fabricated 3D NPS-self-doped carbon foam (NPS-CFs) anodes by direct pyrolysis of commercial bread could yield abundant macroporous structures with a large surface area (295.07 m^2/g) and excellent conductivity as free-standing anodes for enhanced microbial attachments in MFCs. The maximum power output by NPS-CFs (3134 mW/m^2) that could be obtained was 2.57-fold that of the bare CC anodes (1218 mW/m^2) [11]. However, the disadvantages of 3D carbon nanoporous anodes, owing to complicated preparation methods, prevent their extensive use for practical engineering. Table 2 represents biomass-derived free-standing three-dimensional porous carbon anodes.

Table 2. Biomass-derived free-standing three-dimensional porous carbon anodes.

Free-Standing Anode	Structural Properties	MFCs Type	Anode Reactor Size	Inoculum	Power Output	Refs.
Basswood	3D porous structure with mechanically strong pores	Double-chamber	30 mL	*S. oneidensis* MR-1	483 mW m^{-2}	[10]

Table 2. *Cont.*

Free-Standing Anode	Structural Properties	MFCs Type	Anode Reactor Size	Inoculum	Power Output	Refs.
Bacterial cellulose	Hierarchical mesopores structure	Double-chamber	100 mL	*S. putrefaciens* CN32	1747 mW m^{-2}	[24]
Chestnut shells	Hierarchical porous structure	Single-chamber	28 mL	The effluent of an MFC anolyte	759 mW m^{-2}	[27]
Spirogyra algae	3D micro-tube carbon belt structure	Double-chamber	30 mL	*S. oneidensis* MR-1	408 mW m^{-2}	[48]
Natural kapok fibers	A lightweight 3D hollow structure	Single-chamber	28 mL	Anaerobic sludge	1738.1 mW m^{-2}	[49]
Pine cone	3D N, P-codoped macroporous	Double-chamber	100 mL	A mixture of bacteria-enriched effluent and anaerobic sludge	10,880 mW m^{-3}	[50]
Lodgepole pine wood chips	Solid architecture biochar	Double-chamber	200 mL	Anaerobic sludge	532 mW m^{-2}	[43]
Tubular bamboo charcoal	N-enriched carbon anode	Double-chamber	63 mL	Anaerobic effluent	1652 mW m^{-2}	[51]
Loofah sponge	3D macroporous	Single-chamber	21 mL	Wastewater	4083 mW m^{-3}	[52]
Sewage sludge	Highly carbon content	Double-chamber	45 mL	The effluent of a reactor rich in *Geobacter*	2228 mW m^{-2}	[53]
Sugarcane	3D macroporous	Double-chamber	80 mL	Effluent from MFCs	59,940 mW m^{-3}	[54]

2.3. Biomass-Derived Carbons for Hybrid Structured Carbon Anodes

Similarly, incorporating some carbon composites such as carbon nanotubes (CNTs) on biomass surfaces with 3D porous structures is a simple and effective technique to develop highly conductive 3D free-standing carbon-based MFC anodes [28,55]. For example, the fabricated two-scale porous anode from a simple dipping-drying process of CNT ink on macroscale porous textiles made of intertwined polyester fibers could develop CNT textile fiber anodes with diameters of approximately 20 μm of open 3D sites for effective substrate delivery and interior microbial colonization [56]. The modeled CNT textile anodes in MFCs resulted in a 68% increase in maximum power density as compared to the CC anode [56]. Nevertheless, the nonconductivity of the biomass caused by direct processing without calcination may adversely impact the performance of the MFCs [28].

In this instance, Wang et al. pyrolyzed corncob biomass, and then PANI and PPy were coated as external N-precursors during the fabrication of 3D N-doped macroporous carbon foams (NMCFs) to enrich the N-doped state of the carbonized corncob. The sample was further treated with the same pyrolysis method to obtain the corresponding anodes. Their finding revealed that the MFCs with PPy@NMCF-1000 anodes represented a remarkable performance among the MFCs with different NMCF anodes [57]. Moreover, biomass derivatives could also be incorporated to develop anodes for improved efficiency of MFCs. For example, Katuri et al. designed 3D monoliths microchanelled scaffold (MWCNT/CHI) anodes composed of multiwall CNTs (MWCNTs) and chitosan (CHI) as a derivative of shellfish biomass skeletons. The hierarchically porous MWCNT/CHI provided a high surface-area-to-volume ratio with an average channel size of about 16 μm, ideal for microbial colonization in the interior of the MWCNT/CHI anodes, which resulted in a maximum volumetric power density of 2.87 W m^{-2} [58]. In another study, the prepared graphene oxide (GO) from the empty fruit bunch–derived lignin was used as a carbon anode for cobalt (II) remediation in synthesized wastewater. The pure GO-coated graphite rods with and without TiO_2 metal oxide were used to fabricate anodes with higher conductivity and a larger surface area. The resulting power output in the GO/TiO_2 anodes was 5.7 times

higher than that of the pure GO anodes in MFCs [59]. It revealed that the significance of the hybrid anode structure of the biomass/derivative carbon materials incorporated with metal nanocomposites is beneficial for improving the efficiency of MFCs. Nevertheless, the production of nanostructured carbons (e.g., GO, fullerenes, CNTs, etc.), owing to insufficient raw resources, harsh preparation conditions (T > 5000 °C), and the costly procedure, are complicated, resulting in a low production yield [30,37,60–62]. Table 3 represents biomass-derived hybrid structured carbon anodes.

Table 3. Biomass-derived hybrid structured carbon anodes.

Hybrid Anode	Structural Properties	MFCs Type	Anode Reactor Size	Inoculum	Power Output	Refs.
PPy/Corncob	3D N-doped	Double-chamber	80 mL	Anaerobic sludge	4990 mW m^{-2}	[57]
Sewage sludge/Fly ash	Quasi-spherical	Double-chamber	45 mL	Sewage sludge	3200 mW m^{-2}	[63]
Carbon black/ Loofah sponge	Inherent 3D hierarchical macroporous	Double-chamber	25 mL	Effluent from active acetate-fed MFCs	61.7 mW cm^{-3}	[64]
PANI/ Steamed cake	Hierarchically structured 3D macroporous	Single-chamber	30 mL	Sewage sludge	1307 mW m^{-2}	[65]
PPy/ Municipal sludge	Porous structure and abundant in functional group	Double-chamber	25 mL	*S. oneidensis* MR-1	568.5 mW m^{-2}	[66]
PEDOT/$NiFe_2O_4$/ Neem wood	Tunnel structure	Double-chamber	N/A	Pre-acclimated wastewater from MFCs	256 mW m^{-2}	[67]
TiO_2/Egg-white protein/Loofah sponge carbon	Nano-structured capacitive layer coated 3D anode	Single-chamber	28 mL	Activated anaerobic sludge	2590 mW m^{-2}	[68]
NRGO/ CeO_2 nanotubes /Waste tissue paper	3D carbon aerogel	Double-chamber	N/A	Pre-acclimated wastewater	152 mW m^{-2}	[69]
Cellulose/ NaOH-urea aerogel	Hierarchical porous carbon	Double-chamber	100 mL	*S. putrefaciens* CN32	446 mW cm^{-2}	[70]
Chinese ink/ Loofah sponge	3D macroporous	Single-chamber	1000 mL	Pre-acclimated bacteria from other MFCs	0.82 mW cm^{-3}	[71]

3. Morphology of Biomass-Derived Carbon Anodes

Biomass can be transformed into various morphologically structured carbon materials. The different shapes of carbon materials, with their incomparable mechanical stability and conductivity, can potentially impact the optimal performance of MFCs. On the other hand, the different morphologies of the biomass precursors can result in various electrochemical performances. Thus, the development of carbon anodes with adjustable morphologies was suggested to enhance electrochemical capabilities [33]. Diverse parameters such as type of biomass, carbonization and fabrication process, carbonization time, carbonization temperature, and activation process can influence the morphology of biomass-derived carbons [72]. Herein, the most morphologically derived MFC carbon anodes from biomass are addressed.

Lightweight, fibrous, hollow/tubular carbons are unique among other porous and 3D carbon anode materials, providing exterior and interior surfaces suitable for electron transfer. Unlike all other morphologies of carbon anodes, the specific surface area for electron transportation is limited on the exterior surface [49]. Zhu et al. tailored a novel hollow

natural fiber MFC anode using natural kapok fiber biomass. The hollow structured anode resulted in double surfaces from internal and external hollows, which was beneficial for durable microbial attachment and enhanced electricity production in MFCs. The normalized power density by mass using the hollow carbon anodes (104.1 mW g^{-1}) was obtained 20 times higher than that of a traditional carbon cloth anode (5.5 mW g^{-1}) [49] (Figure 1a–d). Additionally, in another study by Shi et al., *spirogyra* algae filaments with fibrous microtube structures could form a lightweight, 3D, non-woven and interconnected macroporous carbon belt anode [48] (Figure 2a–d). The naturally obtained carbon nanoparticles after carbonization on the surface of the anode from the elemental presence of carbohydrates or amino acids in *spirogyra* could greatly enlarge the specific surface area to facilitate enriched biofilm formation for improved EET kinetics in MFCs [48]. Further, it was reported that the inner diameter of the tubes in the carbon anodes is one of the key factors influencing the electron mass transfer in the inner portion of the tube [73]. Li et al. examined the impact of internal diameter (i.e., D1 mm, D1.5 mm, D2 mm, D3 mm) of bamboo charcoal tubes as MFC anodes for both short-term (after a successful start-up) and long-term operation (after operation for 30 days). Unlike D1 mm and D1.5 mm anodes, the voltage output of MFCs with D2 and D3 showed a stable performance after long-term operation, whereas the resulting compact and thicker biofilm of the MFCs with D1 and D1.5 anodes clogged the inner side and increased the internal resistance of the MFCs [73] (Figure 3a–d).

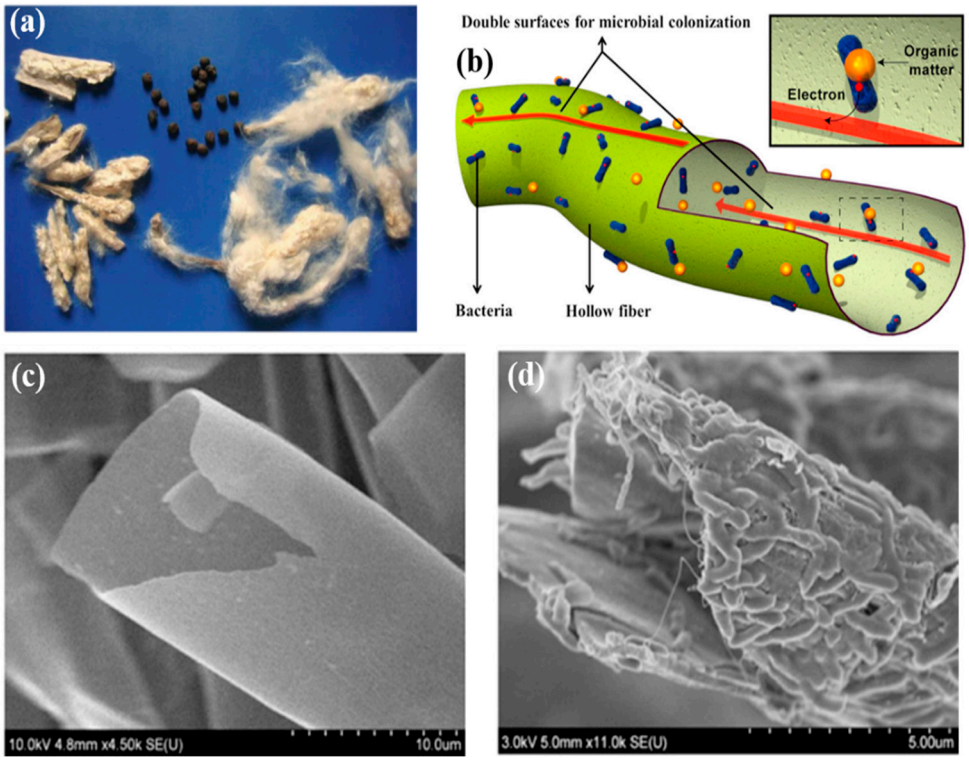

Figure 1. (**a**) The image of the kapok fibers and the seeds from the kapok seed husks. (**b**) The schematic displays the hollow kapok fiber as the anode support for microbial development and offers double surfaces for microbial attachments through both interior and exterior surfaces. The kapok fiber employed in the MFCs is post-carbonization with outstanding conductivity. Notably, bacteria could grow inside and outside the hollow fiber, maximizing the direct contact of exoelectrogens with the conductive fiber surface. (**c**) Images of the kapok fiber morphology after carbonization and (**d**) SEM images of the microbial development on the kapok fiber. (Reproduced with permission: Copyright 2014, Elsevier) [49].

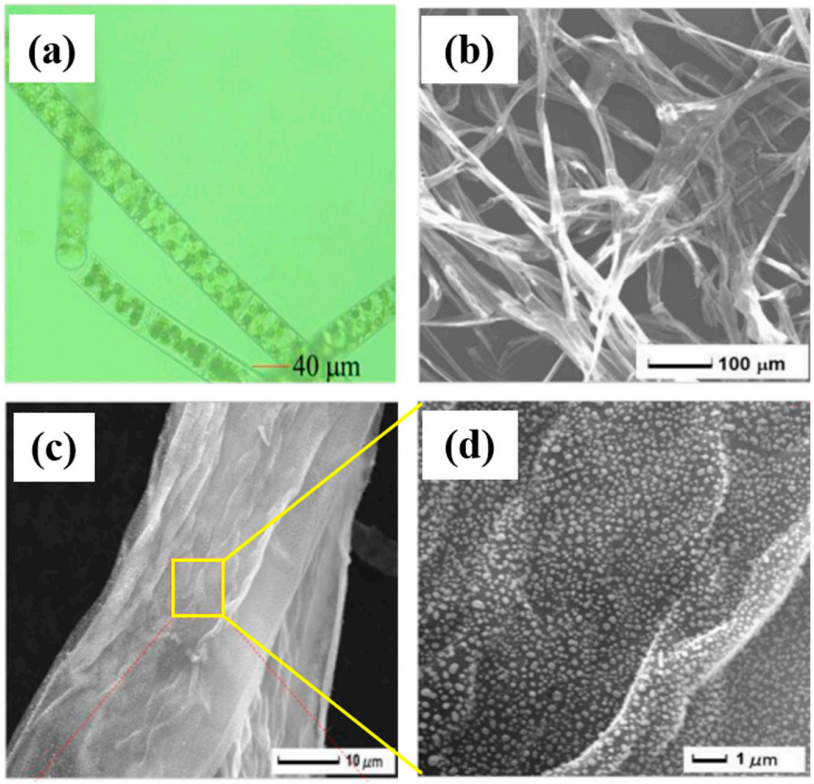

Figure 2. (**a**) Microscopic image of fresh *spirogyra* filaments (fibrous micro-tube structures), (**b**) SEM image of the *spirogyra* carbon belt, (**c**) SEM image of single *spirogyra* carbon belt, (**d**) interior SEM image of the selected area of *spirogyra* carbon belt in image (**c**). (Reproduced with permission: Copyright 2019, RSC) [48].

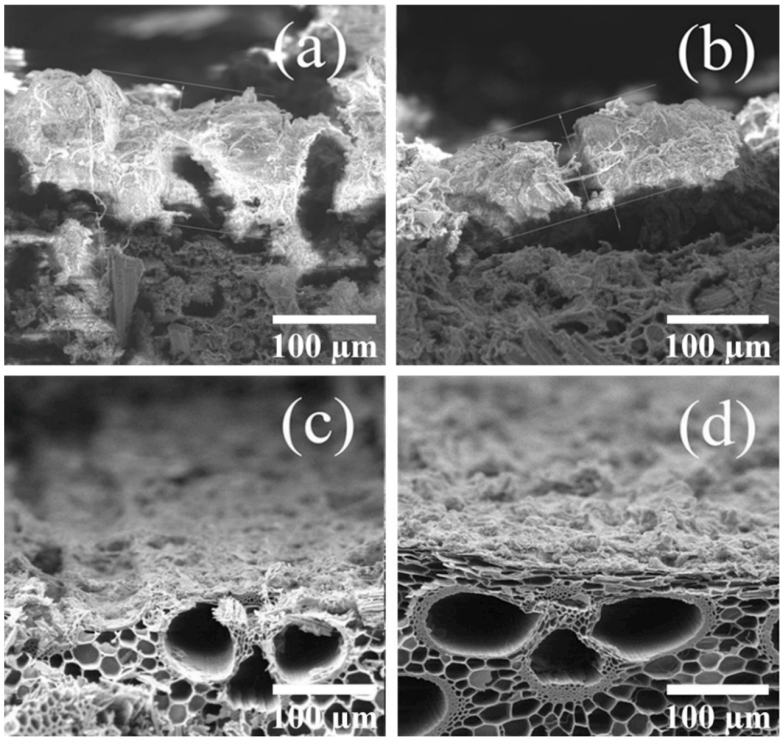

Figure 3. SEM images of the inlet cross-section of tubes with an internal diameter of 1 mm (**a**), 1.5 mm (**b**), 2 mm (**c**), and 3 mm (**d**) after 35 days of operation (×500). (Reproduced with permission: Copyright 2014, Elsevier) [73].

Spherical carbons are drawing considerable interest due to their several potential advantages over other forms of carbon, including excellent durability, exceptional mechanical strength, high adsorption capacity, high bulk density, and controlled pore size distribution to harvest higher volume energy density in MFCs [33,72]. Spherical morphology is ideal for high specific capacitance and prolonged cycling stability [33]. It was reported that fly ash, a major solid waste from coal-fired power stations, can increase the mechanical strength and influence the graphitization of spherical carbon materials [63]. In a study by Jia et al., the synthesized onion-shaped carbon anodes (a type of quasi-spherical anode) from sewage sludge with 20% fly ash as a binder demonstrated 18-fold higher mechanical strength than that of the MFC anodes without fly ash, which specified an excellent stability potential of the anodes for a long-term MFC operation [63] (Figure 4a–c). Similarly, Chen et al. developed a novel, hierarchically 3D-structured microscopic/macroscopic urchin-like carbon anode using chestnut shells (CSEs). CSEs with and without thorns were carbonized to fabricate carbon sphere anodes. Upon MFC performance, the maximum power density with the CSEs (759 mW m^{-2}) was higher than that of the thornless CSEs (425 mW m^{-2}), in which the urchin-like carbon anodes with dense and hard thorns extending out on the spherical shell, signified a crucial role for thorns in increasing specific electrochemically active sites for microbial immobilizing without clogging issues during biofilm formation [27]. Synthesized candle soot, as an alternative to commercial graphite, for MFC anode materials displayed spherical-like carbon nanoparticles (CNPs) pronged through small nanotube-like structures. Similarly, owing to robust particle diffusive bonding, the CNPs exhibited excellent mechanical stability and adhesive properties for excellent microbial attachment [38] (Figure 5a–d).

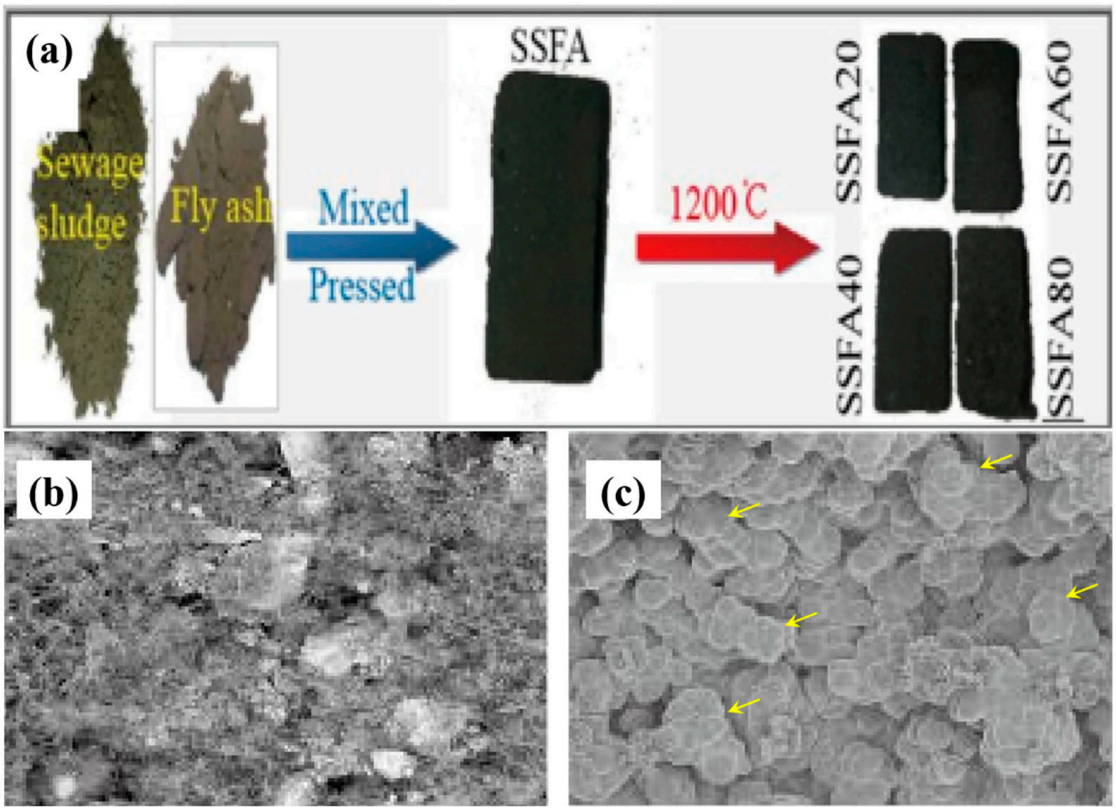

Figure 4. (**a**) The schematic of the sewage sludge/ash (SSA) anode procedure with different ash ratios. The SEM images (500 nm) of (**b**) SSFA0 and (**c**) SSFA20. (Reproduced with permission (The yellow arrows show the quasi-spherical-shaped SSA carbon): Copyright 2018, Elsevier) [63].

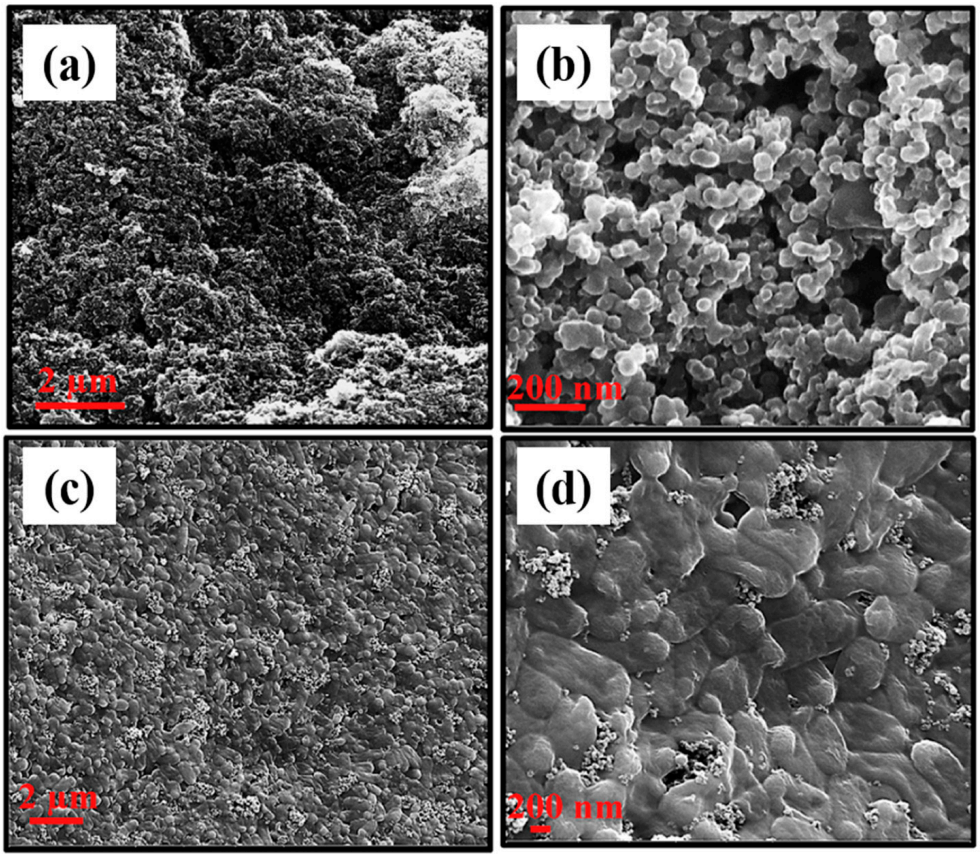

Figure 5. (**a**,**b**) The SEM of bared CNP anode. (**c**,**d**) Dense and uniform biofilm formation on CNP-based anode after 5 days. (Reproduced with permission: Copyright 2018, Elsevier) [38].

Thin, sheet-like carbons with large lateral shapes and exceptional layered structure provide an abundance of specific electrochemically active sites for ion adsorption/desorption with reduced ion diffusion paths [33]. It was reported that thermal treatment, template, and carbonization-activation processes could convert biomass into sheet-like carbons [33]. According to Xu et al., the hydrothermal carbonization using HAc could exfoliate graphene-like, thin nanosheets from the surface of natural basswood with the potential of hydrolyzing polymeric cellulose into oligosaccharides [10]. The combination of HAc and H_2O_2 in the hydrothermal process produced rich nanopores on the surface channels, enlarging the surface area for biofilm growth and further offering steric sites for multi-transportation paths of electrons, ions, nutrients, and cells [10] (Figure 6a–g).

Inherent hierarchical carbons, owing to their inherent 3D interconnected porous/channel structure and a large specific surface site, can amplify electron mass transfer, reduce ion transportation paths, and minimize internal resistance in MFCs [33]. The carbon anode from the natural biomass of almond shells with the inherent hierarchical porous structure showed interconnected macropores and mesopores with a high specific surface area (616.04 $m^2\ g^{-1}$), resulting in superior microbial attachment with a maximum power density of 4346 mW m^{-2} in MFCs [39] (Figure 7a–d). Pine cone–derived carbon anodes with N, P-codoped macroporous structures lead to a fast start-up of cells and long-term cycling stability in MFCs. The charge transfer resistance (1.4 Ω) observed was 85.1% lower than the carbon felt anode, which is beneficial for high conductivity and enhanced EET kinetics [50]. The fabrication of a new carbon anode with depositing H_2O_2-treated carbon black nanocomposite on the surface of the inherent 3D macroporous structured loofah sponge increased the mechanical strength and the surface functional groups for superior MFC performance and resulted in a 17% higher maximum power output (61.7 W m^{-3}) than that of the untreated carbon black/LS [64] (Figure 8a–e).

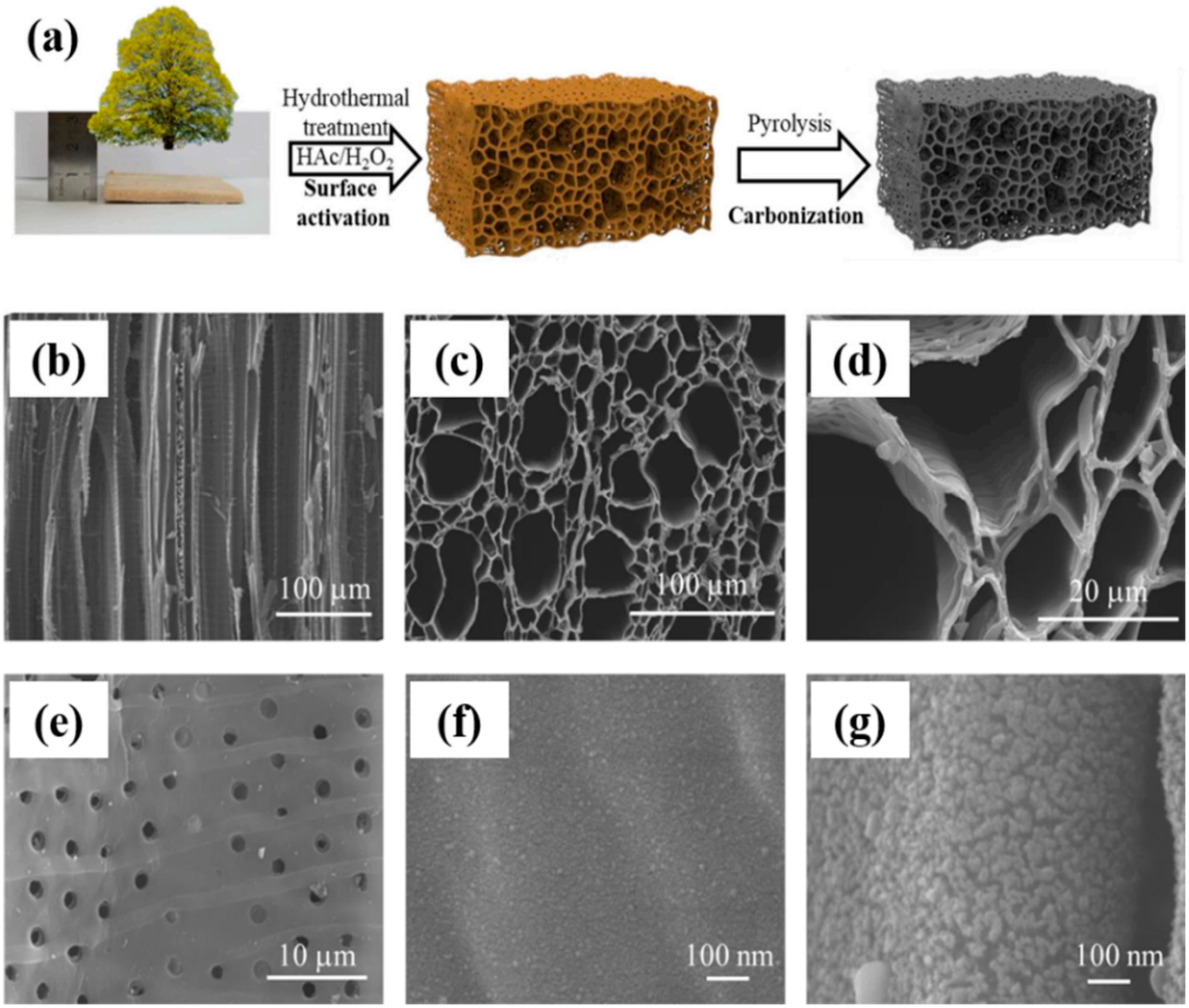

Figure 6. (**a**) Schematic of the 3D hierarchically porous and surface-activated wood anode. (**b**–**e**). The scanning electron microscope images of the wood anode for the observation of straight channels (**b**), macropores (**c**,**d**), and mesopores (**e**). (**f**,**g**). The observation of the surface morphology of the wood anodes without pretreatment (**f**) or with pretreatment (**g**). (Reproduced with permission: Copyright 2022, Wiley) [10].

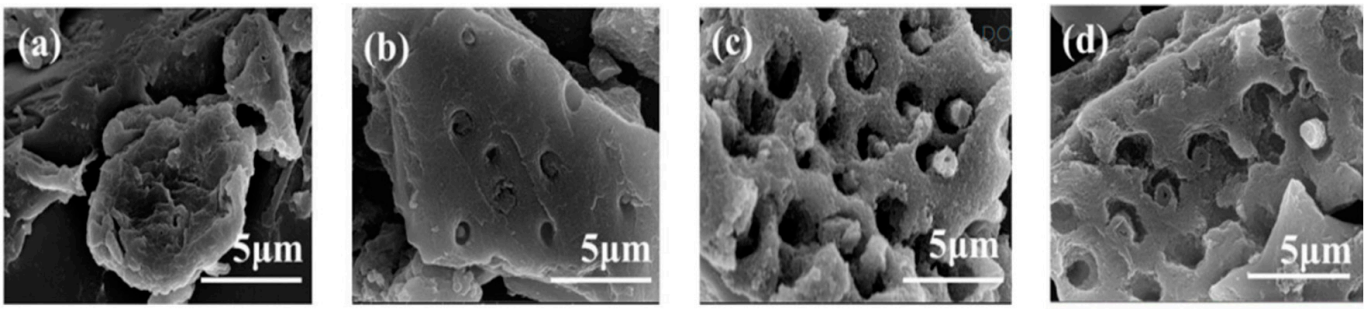

Figure 7. The SEM images of (**a**) carbon material from a raw almond shell, (**b**) porous carbon (PC) PC-600, (**c**) PC-800, and (**d**) PC-1000. (Reproduced with permission: Copyright 2021, RSC) [39].

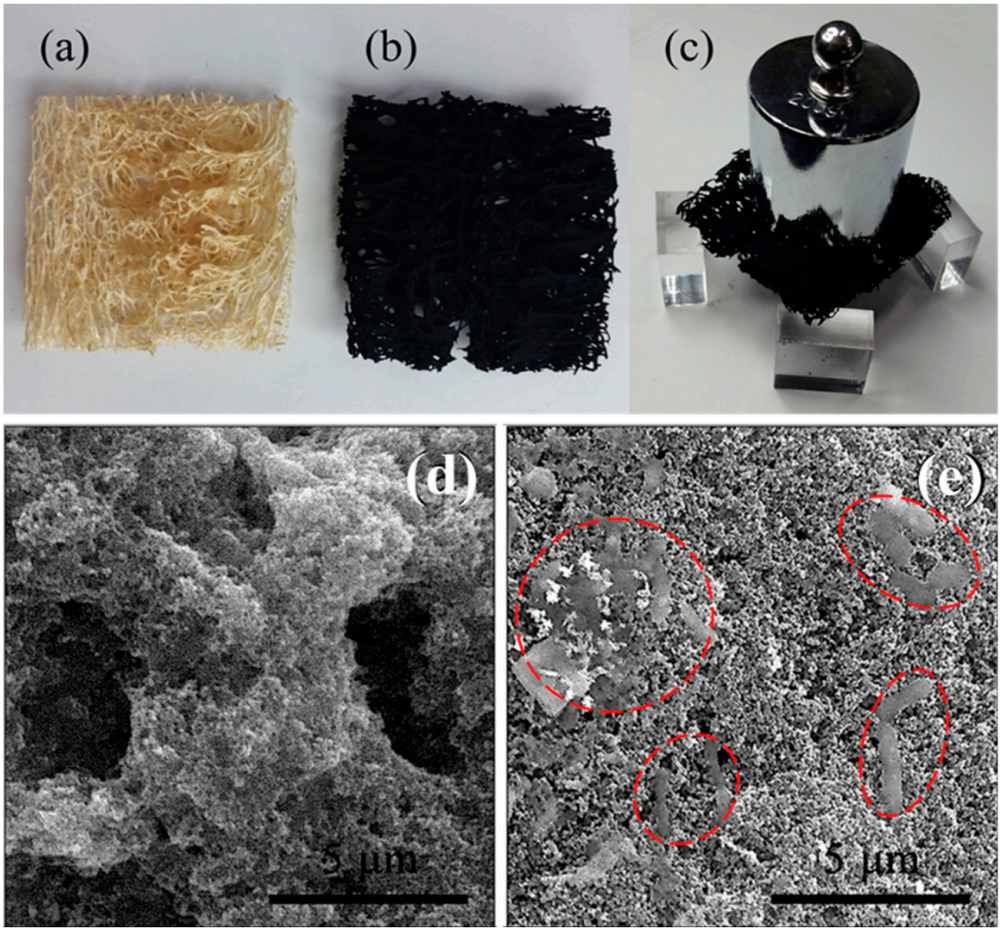

Figure 8. (**a**) The image of the loofah sponge, (**b**) Carbon black-coated loofah sponge anode, and (**c**) The mechanical strength of carbon black-coated loofah sponge anode supporting 200 g (ca. 400 times the weight of LS), (**d**) Biofilm formation on unmodified, and (**e**) The H_2O_2 treated carbon black surface (The red circles show the compact structure of microbial attachment on H_2O_2 treated carbon black) (Reproduced with permission: Copyright 2021, RSC) [64].

4. Strategies for the Fabrication Process of Biomass-Derived Anodes

To increase the specific surface sites, porosity, and conductivity in carbon anodes based on biomass type, certain facile and sustainable strategies, including activation (i.e., physical, chemical), hydrothermal carbonization, and molten salt carbonization have already been discussed [33,35,74]. For example, hierarchical AC nanocomposites from biomass precursors with possession of high specific surface sites and rich pore structures are used for anodes in MFCs, but typically the capacity of these carbon anodes is limited by the micropore structure and relatively low conductivity at high current density [75,76]. Therefore, the biomass type along with an effective technique for the controllable anode fabrication process should be considered in terms of enhanced electrochemical properties. For example, due to the difficulty of obtaining a suitably large surface site in lignocellulosic biomass such as straws, carbonization and activation through a two-step physical and chemical process were suggested to enhance the mesoporous structure in straw-derived carbon material [77].

Physical activation is a thermal carbonization procedure for producing carbonized anodes in an inert atmosphere such as CO_2, N_2, or steam (H_2O) as the pyrolysis agent, inducing the deletion of carbon atoms and aiding in the formation of a porous structure. However, when steam and a gas carrier are combined for physical activation, it poses a technical challenge because the activation process demands a higher temperature [74,75,77]. Yang et al. fabricated a biochar-based packed anode from raw cocklebur fruits by a one-step pyrolysis at 900 °C under an N_2 atmosphere without pre- or post-treatment. The obtained

activated biochar presented a rough surface with thorns all around and a relatively high graphitic degree and porous structure [40]. Nevertheless, adopting physical activation alone (direct pyrolysis) is inefficient in terms of time, high energy costs, and environmental compatibility [78].

Similarly, during the pyrolysis process, heteroatoms in some natural biomass react as natural dopants, triggering in situ self-doped carbon for improved storage sites and diffusion kinetics, whereas water evaporation following high temperature results in the development of a porous structure in carbon nanocomposites [30]. The obtained 3D NMCFs from naturally abundant nitrogenous corncobs incorporated PPy (PPy/NMCF) by a one-step pyrolysis process at 1000 °C with a high purity Ar atmosphere resulted in a high surface area of 589.38 m^2 g^{-1} and macroporous volume of 3.03 cm^3 g^{-1}, which was higher than that of the NMCF anode without PPy (443.44 m^2 g^{-1} and 2.13 cm^3 g^{-1}, respectively) [57].

Chemical activation, either by using strong acids (e.g., H_3PO_4, H_2SO_4, HNO_3, etc.) or alkalis (e.g., KOH and NaOH, among others) with the advantages of a lower pyrolytic temperature, shorter time of pyrolysis, higher carbon yield, and greater specific surface area, which results in oxidation and dehydrogenation during pyrolysis process, leads to a disordering structure and pore formation [76]. The activated carbon anode from silver grass with KOH activation at 900 °C in an inert N_2 atmosphere resulted in an excellent surface area of 3027 m^2 g^{-1}, resulting in a synergistic effect from a well-defined micro/meso/macroporous structure with a remarkable EET performance and a maximum power density of 963 mW cm^{-2} in MFCs [41]. Conversely, chemically activated carbon anodes have low conductivity and density, resulting in a low volumetric energy density in MFCs.

Hydrothermal carbonization, also known as a thermochemical treatment, involves a closed system for the thermochemical conversion of biomass into carbon materials in an aqueous solution and under an inert atmosphere at a temperature above 100 °C and pressure over 1 atm [31]. The prepared carbon anodes with this carbonization method have coal-like characteristics, which is ideal for converting cellulosic biomass into carbon anodes [74,78]. The surface-activated wood carbon anode from hydrothermal treatment and mixed H_2O_2 and HAc (*v*: 1:1)-assisting agents resulted in self-constructed and uniformly distributed nanoparticles, macro/mesonanopores, and straight channels, which obtained 8.3 times higher power output in MFCs and 3.1 times higher formic acid production in MEC systems compared to the traditional CC anodes [10]. Nevertheless, the shortcomings of hydrothermal carbonization involved fewer pores and low specific surface area, which may not be a desirable method for competent anode carbon preparation [78].

Molten salt carbonization as a controlled carbonization method is a heating reaction above the melting point of a low melting temperature salt (e.g., NaCl, KCl, $ZnCl_2$, etc.) with a reactant to attain a completely homogeneous carbon nanocomposite [79]. The carbonization using this method offers a higher heat capacity compared to the hydrothermal treatment and maintains the mechanical stability of the carbon material against shrinking, which results in a high mass yield [74]. Li et al. used $ZnCl_2$ as molten salt for porous carbon synthesis from almond shells. The prepared carbon material with a yield of 17% performed macroporous structure attributed to the etching of the Zn^{2+} under high annealing temperature (800 °C), with pore size between 1 and 2 µm [39]. Nevertheless, the carbonization process by molten salt leads to high costs associated with milling and contamination caused by the wear of the milling medium [79].

5. Conclusions and Future Trends

Microbial-operated fuel cells are an attractive energy-producing technology since they can degrade a variety of waste and produce useful energy forms. Among the constructive factors in MFCs, the anode materials with their surface properties, structural characteristics, and morphology can directly influence the performance of MFCs. Although commercial anode materials with good conductivity are typically employed in MFCs, their high cost

and poor power output limit their engineering application in MFCs. To date, research has been conducted on developing anodes for large surface areas, high electrical conductivity, biocompatibility, etc. to improve the shortcomings of power output in MFCs. Regarding this, the strategy of developing carbon anodes from biomass, with its abundant availability, as an alternative to commercial materials has shed light on low-cost and high-value-added anode materials for sustainable and green energy production.

This article reviewed the three designs for biomass-derived carbon anodes based on their final products, including nanocomposite carbons for the surface modification of commercial carbon material, biomass-derived free-standing carbons, and biomass-derived carbons for hybrid structured anodes. The insights on the advantages and disadvantages of each design are highlighted. Further, the characteristics and effects of each carbon anode design based on varied morphology, specific surface area, porous structure, heteroatom doping, graphitization rate, etc. on the performance of MFCs are discussed. For example, the pore structures (micro/meso/macroporous) in carbon anodes play an important role in microbial attachment, EET kinetics, ion diffusion, substrate delivery, and clogging issues. Therefore, the insights into the fabrication process of biomass-derived carbon anodes for controllable carbonized structures should be addressed for enhanced electrochemical properties in MFCs. Similarly, an intensive heat-treatment procedure is usually required to fabricate carbon anodes from biomass materials and control the functionality of the carbon anodes, challenging the practical application of biomass-derived carbon anodes with high carbonization costs. As heat-treatment is an important factor, future research should invent alternative methods to reduce the preparation costs of biomass-derived carbon anodes and control the material features including morphology, porosity, specific surface area, and surface functionality. Typically, nanocomposite carbon anodes require binding agents to form anodes, which adversely impacts anode stability and biocompatibility. Meanwhile, future research should investigate developing advanced binder materials from biomass, improving the efficiency of MFCs and facile anode fabrication for practical application. Additionally, an advanced fabrication method employing enzymes for carbon material activation could be a novel technique to provide cost-effective and green materials. Another investigation should focus on preparing metal organic framework (MOFs)–derived biomass, which would enhance the anode catalysis efficiency for the hydrogenation/oxidation of wastes in MFCs.

Author Contributions: Writing—original draft, J.M.M.; Writing—review and editing, S.W., and A.A.; Validation, J.L.; Visualization, H.W.; Supervision and funding acquisition, J.M. The manuscript was written through the contributions of all authors. All authors have read and agreed to the published version of the manuscript.

Funding: This work is supported by the Innovation Program for Carbon Neutralization of Jiangsu Province (BK20220003).

Conflicts of Interest: The authors declare no conflict of interest.

Abbreviations

BESs	bioelectrochemical systems
MECs	microbial electrolysis cells
MFCs	microbial fuel cells
CC	carbon cloth
CF	carbon felt
EET	extracellular electron transfer
3D	three-dimensional
CWACs	coffee waste-derived activated carbons
ACs	activated carbons
2D	two-dimensional
CB	carbon brush

CNTs	carbon nanotubes
NMCFs	N-doped macroporous carbon foams
MWCNTs	multiwall carbon nanotubes
CHI	chitosan
GO	graphene oxide
CSEs	chestnut shells
CNPs	carbon nanoparticles
PC	porous carbon

References

1. Sun, Y.; Shi, X.L.; Yang, Y.L.; Suo, G.; Zhang, L.; Lu, S.; Chen, Z.G. Biomass-Derived Carbon for High-Performance Batteries: From Structure to Properties. *Adv. Funct. Mater.* **2022**, *8*, 2201584. [CrossRef]
2. Liu, J.; Yong, Y.-C.; Song, H.; Li, C.M. Activation enhancement of citric acid cycle to promote bioelectrocatalytic activity of arcA knockout Escherichia coli toward high-performance microbial fuel cell. *ACS Catal.* **2012**, *2*, 1749–1752. [CrossRef]
3. Moradian, J.M.; Fang, Z.; Yong, Y.-C. Recent advances on biomass-fueled microbial fuel cell. *Bioresour. Bioprocess.* **2021**, *8*, 14. [CrossRef]
4. Wang, J.-X.; Yang, X.-J.; Wang, Y.-Z.; Yang, K.; Chen, H.; Yong, Y.-C. Bio-Nanohybrid Cell Based Signal Amplification System for Electrochemical Sensing. *Anal. Chem.* **2022**, *94*, 7738–7742. [CrossRef]
5. Yang, Y.; Yu, Y.-Y.; Shi, Y.-T.; Moradian, J.M.; Yong, Y.-C. In Vivo Two-Way Redox Cycling System for Independent Duplexed Electrochemical Signal Amplification. *Anal. Chem.* **2019**, *91*, 4939–4942. [CrossRef]
6. Yu, Y.-Y.; Wang, Y.-Z.; Fang, Z.; Shi, Y.-T.; Cheng, Q.-W.; Chen, Y.-X.; Shi, W.; Yong, Y.-C. Single cell electron collectors for highly efficient wiring-up electronic abiotic/biotic interfaces. *Nat. Commun.* **2020**, *11*, 4087. [CrossRef]
7. Cai, T.; Meng, L.; Chen, G.; Xi, Y.; Jiang, N.; Song, J.; Zheng, S.; Liu, Y.; Zhen, G.; Huang, M. Application of advanced anodes in microbial fuel cells for power generation: A review. *Chemosphere* **2020**, *248*, 125985. [CrossRef] [PubMed]
8. Bruzaite, I.; Rozene, J.; Morkvenaite-Vilkonciene, I.; Ramanavicius, A. Towards microorganism-based biofuel cells: The viability of saccharomyces cerevisiae modified by multiwalled carbon nanotubes. *Nanomaterials* **2020**, *10*, 954. [CrossRef]
9. Zinovicius, A.; Rozene, J.; Merkelis, T.; Bruzaite, I.; Ramanavicius, A.; Morkvenaite-Vilkonciene, I. Evaluation of a yeast–polypyrrole biocomposite used in microbial fuel cells. *Sensors* **2022**, *22*, 327. [CrossRef] [PubMed]
10. Xu, Z.A.; Ma, X.M.; Shi, Y.T.; Moradian, J.M.; Wang, Y.Z.; Sun, G.F.; Du, J.; Ye, X.M.; Yong, Y.C. Surface activated natural wood biomass electrode for efficient microbial electrocatalysis: Performance and mechanism. *Int. J. Energy Res.* **2022**, *46*, 8480–8490. [CrossRef]
11. Zhang, L.; He, W.; Yang, J.; Sun, J.; Li, H.; Han, B.; Zhao, S.; Shi, Y.; Feng, Y.; Tang, Z. Bread-derived 3D macroporous carbon foams as high performance free-standing anode in microbial fuel cells. *Biosens. Bioelectron.* **2018**, *122*, 217–223. [CrossRef] [PubMed]
12. Ali, A.; Naveed, A.; Shehzad, K.; Aziz, T.; Rasheed, T.; Moradian, J.M.; Hassan, M.; Rahman, A.; Zhiqiang, F.; Guo, L. Polymerization kinetics of bicyclic olefins and mechanism with symmetrical ansa-metallocene catalysts associated with active center count: Relationship between their activities and structure and activation path. *RSC Adv.* **2022**, *12*, 15284–15295. [CrossRef] [PubMed]
13. Yong, Y.-C.; Yu, Y.-Y.; Li, C.-M.; Zhong, J.-J.; Song, H. Bioelectricity enhancement via overexpression of quorum sensing system in Pseudomonas aeruginosa-inoculated microbial fuel cells. *Biosens. Bioelectron.* **2011**, *30*, 87–92. [CrossRef] [PubMed]
14. Yong, Y.C.; Yu, Y.Y.; Yang, Y.; Liu, J.; Wang, J.Y.; Song, H. Enhancement of extracellular electron transfer and bioelectricity output by synthetic porin. *Biotechnol. Bioeng.* **2013**, *110*, 408–416. [CrossRef]
15. Moradian, J.M.; Xu, Z.A.; Shi, Y.T.; Fang, Z.; Yong, Y.C. Efficient biohydrogen and bioelectricity production from xylose by microbial fuel cell with newly isolated yeast of Cystobasidium slooffiae. *Int. J. Energy Res.* **2020**, *44*, 325–333. [CrossRef]
16. Moradian, J.M.; Mi, J.-L.; Dai, X.; Sun, G.-F.; Du, J.; Ye, X.-M.; Yong, Y.-C. Yeast-induced formation of graphene hydrogels anode for efficient xylose-fueled microbial fuel cells. *Chemosphere* **2021**, *291*, 132963. [CrossRef]
17. Yong, Y.C.; Yu, Y.Y.; Zhang, X.; Song, H. Highly active bidirectional electron transfer by a self-assembled electroactive reduced-graphene-oxide-hybridized biofilm. *Angew. Chem. Int. Ed.* **2014**, *53*, 4480–4483. [CrossRef]
18. Moradian, J.M.; Yang, F.-Q.; Xu, N.; Wang, J.-Y.; Wang, J.-X.; Sha, C.; Ali, A.; Yong, Y.-C. Enhancement of bioelectricity and hydrogen production from xylose by a nanofiber polyaniline modified anode with yeast microbial fuel cell. *Fuel* **2022**, *326*, 125056. [CrossRef]
19. Yong, Y.-C.; Dong, X.-C.; Chan-Park, M.B.; Song, H.; Chen, P. Macroporous and monolithic anode based on polyaniline hybridized three-dimensional graphene for high-performance microbial fuel cells. *ACS Nano* **2012**, *6*, 2394–2400. [CrossRef]
20. Pocaznoi, D.; Calmet, A.; Etcheverry, L.; Erable, B.; Bergel, A. Stainless steel is a promising electrode material for anodes of microbial fuel cells. *Energy Environ. Sci.* **2012**, *5*, 9645–9652. [CrossRef]
21. Qiao, Y.; Wu, X.-S.; Ma, C.-X.; He, H.; Li, C.M. A hierarchical porous graphene/nickel anode that simultaneously boosts the bio-and electro-catalysis for high-performance microbial fuel cells. *Rsc Adv.* **2014**, *4*, 21788–21793. [CrossRef]
22. Karthikeyan, R.; Wang, B.; Xuan, J.; Wong, J.W.; Lee, P.K.; Leung, M.K. Interfacial electron transfer and bioelectrocatalysis of carbonized plant material as effective anode of microbial fuel cell. *Electrochim. Acta* **2015**, *157*, 314–323. [CrossRef]

23. Meng, L.; Feng, M.; Sun, J.; Wang, R.; Qu, F.; Yang, C.; Guo, W. High-performance free-standing microbial fuel cell anode derived from Chinese date for enhanced electron transfer rates. *Bioresour. Technol.* **2022**, *353*, 127151. [CrossRef]
24. Zou, L.; Qiao, Y.; Wu, Z.Y.; Wu, X.S.; Xie, J.L.; Yu, S.H.; Guo, J.; Li, C.M. Tailoring unique mesopores of hierarchically porous structures for fast direct electrochemistry in microbial fuel cells. *Adv. Energy Mater.* **2016**, *6*, 1501535. [CrossRef]
25. Lu, M.; Qian, Y.; Yang, C.; Huang, X.; Li, H.; Xie, X.; Huang, L.; Huang, W. Nitrogen-enriched pseudographitic anode derived from silk cocoon with tunable flexibility for microbial fuel cells. *Nano Energy* **2017**, *32*, 382–388. [CrossRef]
26. Chen, Q.; Pu, W.; Hou, H.; Hu, J.; Liu, B.; Li, J.; Cheng, K.; Huang, L.; Yuan, X.; Yang, C. Activated microporous-mesoporous carbon derived from chestnut shell as a sustainable anode material for high performance microbial fuel cells. *Bioresour. Technol.* **2018**, *249*, 567–573. [CrossRef]
27. Chen, S.; Tang, J.; Jing, X.; Liu, Y.; Yuan, Y.; Zhou, S. A hierarchically structured urchin-like anode derived from chestnut shells for microbial energy harvesting. *Electrochim. Acta* **2016**, *212*, 883–889. [CrossRef]
28. Fan, X.; Zhou, Y.; Jin, X.; Song, R.B.; Li, Z.; Zhang, Q. Carbon material-based anodes in the microbial fuel cells. *Carbon Energy* **2021**, *3*, 449–472. [CrossRef]
29. Zhou, M.; Chi, M.; Luo, J.; He, H.; Jin, T. An overview of electrode materials in microbial fuel cells. *J. Power Sources* **2011**, *196*, 4427–4435. [CrossRef]
30. Yang, W.; Chen, S. Biomass-derived carbon for electrode fabrication in microbial fuel cells: A review. *Ind. Eng. Chem. Res.* **2020**, *59*, 6391–6404. [CrossRef]
31. Long, W.; Fang, B.; Ignaszak, A.; Wu, Z.; Wang, Y.-J.; Wilkinson, D. Biomass-derived nanostructured carbons and their composites as anode materials for lithium ion batteries. *Chem. Soc. Rev.* **2017**, *46*, 7176–7190. [CrossRef] [PubMed]
32. Lyu, L.; Seong, K.-D.; Ko, D.; Choi, J.; Lee, C.; Hwang, T.; Cho, Y.; Jin, X.; Zhang, W.; Pang, H. Recent development of biomass-derived carbons and composites as electrode materials for supercapacitors. *Mater. Chem. Front.* **2019**, *3*, 2543–2570. [CrossRef]
33. Luo, X.; Chen, S.; Hu, T.; Chen, Y.; Li, F. Renewable biomass-derived carbons for electrochemical capacitor applications. *SusMat* **2021**, *1*, 211–240. [CrossRef]
34. Hung, Y.-H.; Liu, T.-Y.; Chen, H.-Y. Renewable coffee waste-derived porous carbons as anode materials for high-performance sustainable microbial fuel cells. *ACS Sustain. Chem. Eng.* **2019**, *7*, 16991–16999. [CrossRef]
35. Li, R.; Zhou, Y.; Li, W.; Zhu, J.; Huang, W. Structure engineering in biomass-derived carbon materials for electrochemical energy storage. *Research* **2020**, *2020*, 8685436. [CrossRef] [PubMed]
36. Wang, H.; Davidson, M.; Zuo, Y.; Ren, Z. Recycled tire crumb rubber anodes for sustainable power production in microbial fuel cells. *J. Power Sources* **2011**, *196*, 5863–5866. [CrossRef]
37. Zhu, K.; Xu, Y.; Yang, X.; Fu, W.; Dang, W.; Yuan, J.; Wang, Z. Sludge Derived Carbon Modified Anode in Microbial Fuel Cell for Performance Improvement and Microbial Community Dynamics. *Membranes* **2022**, *12*, 120. [CrossRef]
38. Singh, S.; Bairagi, P.K.; Verma, N. Candle soot-derived carbon nanoparticles: An inexpensive and efficient electrode for microbial fuel cells. *Electrochim. Acta* **2018**, *264*, 119–127. [CrossRef]
39. Li, M.; Ci, S.; Ding, Y.; Wen, Z. Almond shell derived porous carbon for a high-performance anode of microbial fuel cells. *Sustain. Energy Fuels* **2019**, *3*, 3415–3421. [CrossRef]
40. Yang, C.; Chen, M.; Qian, Y.; Zhang, L.; Lu, M.; Xie, X.; Huang, L.; Huang, W. Packed anode derived from cocklebur fruit for improving long-term performance of microbial fuel cells. *Sci. China Mater.* **2019**, *62*, 645–652. [CrossRef]
41. Rethinasabapathy, M.; Lee, J.H.; Roh, K.C.; Kang, S.-M.; Oh, S.Y.; Park, B.; Lee, G.-W.; Cha, Y.L.; Huh, Y.S. Silver grass-derived activated carbon with coexisting micro-, meso-and macropores as excellent bioanodes for microbial colonization and power generation in sustainable microbial fuel cells. *Bioresour. Technol.* **2020**, *300*, 122646. [CrossRef] [PubMed]
42. Ye, W.; Tang, J.; Wang, Y.; Cai, X.; Liu, H.; Lin, J.; Van der Bruggen, B.; Zhou, S. Hierarchically structured carbon materials derived from lotus leaves as efficient electrocatalyst for microbial energy harvesting. *Sci. Total Environ.* **2019**, *666*, 865–874. [CrossRef] [PubMed]
43. Huggins, T.; Wang, H.; Kearns, J.; Jenkins, P.; Ren, Z.J. Biochar as a sustainable electrode material for electricity production in microbial fuel cells. *Bioresour. Technol.* **2014**, *157*, 114–119. [CrossRef]
44. Li, M.; Li, Y.-W.; Cai, Q.-Y.; Zhou, S.-Q.; Mo, C.-H. Spraying carbon powder derived from mango wood biomass as high-performance anode in bio-electrochemical system. *Bioresour. Technol.* **2020**, *300*, 122623. [CrossRef] [PubMed]
45. Dumitru, A.; Scott, K. Anode materials for microbial fuel cells. In *Microbial Electrochemical and Fuel Cells*; Elsevier: Amsterdam, The Netherlands, 2016; pp. 117–152.
46. Ni, H.; Khan, A.; Yang, Z.; Gong, Y.; Ali, G.; Liu, P.; Chen, F.; Li, X. Wood carbon electrode in microbial fuel cell enhances chromium reduction and bioelectricity generation. *Environ. Sci. Pollut. Res.* **2022**, *29*, 13709–13719. [CrossRef]
47. Parlett, C.M.; Wilson, K.; Lee, A.F. Hierarchical porous materials: Catalytic applications. *Chem. Soc. Rev.* **2013**, *42*, 3876–3893. [CrossRef] [PubMed]
48. Shi, Y.-T.; Yu, Y.-Y.; Xu, Z.-A.; Lian, J.; Yong, Y.-C. Superior carbon belts from Spirogyra for efficient extracellular electron transfer and sustainable microbial energy harvesting. *J. Mater. Chem. A* **2019**, *7*, 6930–6938. [CrossRef]
49. Zhu, H.; Wang, H.; Li, Y.; Bao, W.; Fang, Z.; Preston, C.; Vaaland, O.; Ren, Z.; Hu, L. Lightweight, conductive hollow fibers from nature as sustainable electrode materials for microbial energy harvesting. *Nano Energy* **2014**, *10*, 268–276. [CrossRef]

50. Wang, R.; Liu, D.; Yan, M.; Zhang, L.; Chang, W.; Sun, Z.; Liu, S.; Guo, C. Three-dimensional high performance free-standing anode by one-step carbonization of pinecone in microbial fuel cells. *Bioresour. Technol.* **2019**, *292*, 121956. [CrossRef]
51. Zhang, J.; Li, J.; Ye, D.; Zhu, X.; Liao, Q.; Zhang, B. Tubular bamboo charcoal for anode in microbial fuel cells. *J. Power Sources* **2014**, *272*, 277–282. [CrossRef]
52. Zhang, S.; Bao, X.; Wan, F.; Xie, Y.; Liu, Q.; Zhou, B.; Xia, S. Application of loofah sponge three-dimensional cage-shape activated carbon fiber with high strength in an air-cathode microbial fuel cell. *J. Renew. Sustain. Energy* **2018**, *10*, 044301. [CrossRef]
53. Feng, H.; Jia, Y.; Shen, D.; Zhou, Y.; Chen, T.; Chen, W.; Ge, Z.; Zheng, S.; Wang, M. The effect of chemical vapor deposition temperature on the performance of binder-free sewage sludge-derived anodes in microbial fuel cells. *Sci. Total Environ.* **2018**, *635*, 45–52. [CrossRef] [PubMed]
54. Zhou, Y.; Zhou, G.; Yin, L.; Guo, J.; Wan, X.; Shi, H. High-Performance Carbon Anode Derived from Sugarcane for Packed Microbial Fuel Cells. *ChemElectroChem* **2017**, *4*, 168–174. [CrossRef]
55. Aziz, T.; Farid, A.; Haq, F.; Kiran, M.; Ullah, A.; Zhang, K.; Li, C.; Ghazanfar, S.; Sun, H.; Ullah, R.; et al. A Review on the Modification of Cellulose and Its Applications. *Polymers* **2022**, *14*, 3206. [CrossRef] [PubMed]
56. Xie, X.; Hu, L.; Pasta, M.; Wells, G.F.; Kong, D.; Criddle, C.S.; Cui, Y. Three-dimensional carbon nanotube−textile anode for high-performance microbial fuel cells. *Nano Lett.* **2011**, *11*, 291–296. [CrossRef] [PubMed]
57. Wang, Y.; He, C.; Li, W.; Zong, W.; Li, Z.; Yuan, L.; Wang, G.; Mu, Y. High power generation in mixed-culture microbial fuel cells with corncob-derived three-dimensional N-doped bioanodes and the impact of N dopant states. *Chem. Eng. J.* **2020**, *399*, 125848. [CrossRef]
58. Katuri, K.; Ferrer, M.L.; Gutiérrez, M.C.; Jiménez, R.; del Monte, F.; Leech, D. Three-dimensional microchanelled electrodes in flow-through configuration for bioanode formation and current generation. *Energy Environ. Sci.* **2011**, *4*, 4201–4210. [CrossRef]
59. Yaqoob, A.A.; Ibrahim, M.N.M.; Umar, K. Biomass-derived composite anode electrode: Synthesis, characterizations, and application in microbial fuel cells (MFCs). *J. Environ. Chem. Eng.* **2021**, *9*, 106111. [CrossRef]
60. Aziz, T.; Ullah, A.; Ali, A.; Shabeer, M.; Shah, M.N.; Haq, F.; Iqbal, M.; Ullah, R.; Khan, F.U. Manufactures of bio-degradable and bio-based polymers for bio-materials in the pharmaceutical field. *J. Appl. Polym. Sci.* **2022**, *139*, e52624. [CrossRef]
61. Ghosh, S.; Santhosh, R.; Jeniffer, S.; Raghavan, V.; Jacob, G.; Nanaji, K.; Kollu, P.; Jeong, S.K.; Grace, A.N. Natural biomass derived hard carbon and activated carbons as electrochemical supercapacitor electrodes. *Sci. Rep.* **2019**, *9*, 16315. [CrossRef] [PubMed]
62. Liu, Y.; Li, Y.; Gan, R.; Jia, H.; Yong, X.; Yong, Y.-C.; Wu, X.; Wei, P.; Zhou, J. Enhanced biogas production from swine manure anaerobic digestion via in-situ formed graphene in electromethanogenesis system. *Chem. Eng. J.* **2020**, *389*, 124510. [CrossRef]
63. Jia, Y.; Feng, H.; Shen, D.; Zhou, Y.; Chen, T.; Wang, M.; Chen, W.; Ge, Z.; Huang, L.; Zheng, S. High-performance microbial fuel cell anodes obtained from sewage sludge mixed with fly ash. *J. Hazard. Mater.* **2018**, *354*, 27–32. [CrossRef] [PubMed]
64. Zheng, J.; Cheng, C.; Zhang, J.; Wu, X. Appropriate mechanical strength of carbon black-decorated loofah sponge as anode material in microbial fuel cells. *Int. J. Hydrogen Energy* **2016**, *41*, 23156–23163. [CrossRef]
65. Yuan, H.; Dong, G.; Li, D.; Deng, L.; Cheng, P.; Chen, Y. Steamed cake-derived 3D carbon foam with surface anchored carbon nanoparticles as freestanding anodes for high-performance microbial fuel cells. *Sci. Total Environ.* **2018**, *636*, 1081–1088. [CrossRef] [PubMed]
66. Ma, X.; Feng, C.; Zhou, W.; Yu, H. Municipal sludge-derived carbon anode with nitrogen-and oxygen-containing functional groups for high-performance microbial fuel cells. *J. Power Sources* **2016**, *307*, 105–111. [CrossRef]
67. Senthilkumar, N.; Pannipara, M.; Al-Sehemi, A.G. PEDOT/$NiFe_2O_4$ nanocomposites on biochar as a free-standing anode for high-performance and durable microbial fuel cells. *New J. Chem.* **2019**, *43*, 7743–7750. [CrossRef]
68. Tang, J.; Yuan, Y.; Liu, T.; Zhou, S. High-capacity carbon-coated titanium dioxide core–shell nanoparticles modified three dimensional anodes for improved energy output in microbial fuel cells. *J. Power Sources* **2015**, *274*, 170–176. [CrossRef]
69. Senthilkumar, N.; Aziz, M.; Pannipara, M.; Alphonsa, A.T.; Al-Sehemi, A.G.; Balasubramani, A. Waste paper derived three-dimensional carbon aerogel integrated with ceria/nitrogen-doped reduced graphene oxide as freestanding anode for high performance and durable microbial fuel cells. *Bioprocess Biosyst. Eng.* **2020**, *43*, 97–109. [CrossRef] [PubMed]
70. Wang, D.; Wang, Y.; Yang, J.; He, X.; Wang, R.-J.; Lu, Z.-S.; Qiao, Y. Cellulose aerogel derived hierarchical porous carbon for enhancing flavin-based interfacial electron transfer in microbial fuel cells. *Polymers* **2020**, *12*, 664. [CrossRef]
71. Zhou, L.; Sun, L.; Fu, P.; Yang, C.; Yuan, Y. Carbon nanoparticles of Chinese ink-wrapped natural loofah sponge: A low-cost three-dimensional electrode for high-performance microbial energy harvesting. *J. Mater. Chem. A* **2017**, *5*, 14741–14747. [CrossRef]
72. Romero-Anaya, A.J.; Ouzzine, M.; Lillo-Rodenas, M.A.; Linares-Solano, A. Spherical carbons: Synthesis, characterization and activation processes. *Carbon* **2014**, *68*, 296–307. [CrossRef]
73. Li, J.; Zhang, J.; Ye, D.; Zhu, X.; Liao, Q.; Zheng, J. Optimization of inner diameter of tubular bamboo charcoal anode for a microbial fuel cell. *Int. J. Hydrogen Energy* **2014**, *39*, 19242–19248. [CrossRef]
74. Wang, J.; Nie, P.; Ding, B.; Dong, S.; Hao, X.; Dou, H.; Zhang, X. Biomass derived carbon for energy storage devices. *J. Mater. Chem. A* **2017**, *5*, 2411–2428. [CrossRef]
75. Graś, M.; Bartkowiak, M.; Doczekalska, B.; Lota, G. Electrochemical Capacitors Based on Electrodes Made of Lignocellulosic Waste Materials. *Waste Biomass Valorization* **2019**, *11*, 3863–3871.
76. Kim, K.S.; Zhao, Y.; Jang, H.; Lee, S.Y.; Kim, J.M.; Kim, K.S.; Ahn, J.-H.; Kim, P.; Choi, J.-Y.; Hong, B.H. Large-scale pattern growth of graphene films for stretchable transparent electrodes. *Nature* **2009**, *457*, 706–710. [CrossRef] [PubMed]

77. Schröder, E.; Thomauske, K.; Oechsler, B.; Herberger, S.; Baur, S.; Hornung, A. Activated carbon from waste biomass. *Prog. Biomass Bioenergy Prod.* **2011**, 333–356.
78. Gao, Z.; Zhang, Y.; Song, N.; Li, X. Biomass-derived renewable carbon materials for electrochemical energy storage. *Mater. Res. Lett.* **2017**, *5*, 69–88. [CrossRef]
79. Arendt, R.; Rosolowski, J.; Szymaszek, J. Lead zirconate titanate ceramics from molten salt solvent synthesized powders. *Mater. Res. Bull.* **1979**, *14*, 703–709. [CrossRef]